Desorption of Polycyclic Aromatic Hydrocarbons from Soot Surface: Pyrene and Fluoranthene

Angélique Guilloteau,[†,‡] Mai Lan Nguyen,[†] Yuri Bedjanian,*[,†] and Georges Le Bras[†]

Institut de Combustion, Aérothermique, Réactivité et Environnement (ICARE), CNRS, 45071 Orléans Cedex 2, France and Ecole des Mines de Douai, Département Chimie et Environnement, BP 838, 59508 Douai, France

Received: April 8, 2008; Revised Manuscript Received: September 5, 2008

The kinetics of thermal desorption of two four-ring polycyclic aromatic hydrocarbons, fluoranthene, and pyrene from well-characterized laboratory-generated kerosene soot surface was studied over the temperature range 260−320 K in a low-pressure flow reactor combined with an electron-impact mass spectrometer. Two methods were used to measure the desorption rate constants: monitoring of the surface-bound fluoranthene and pyrene decays due to desorption using off-line HPLC measurements of their concentrations in soot samples, and monitoring of the desorbed molecules in the gas phase using in situ mass spectrometric detection. Results obtained with the two methods were in good agreement and yielded the following Arrhenius expressions for the desorption rate constants: k_{des} (fluoranthene) $= 4 \times 10^{14} \exp[-(93900 \pm 1700)/RT]$ and k_{des} (pyrene) $= 6 \times 10^{14} \exp[-(95200 \pm 1800)/RT]$ (k_{des} are in units of s^{-1}, and activation energies are in J mol^{-1}). In addition, the combined uptake coefficient of fluoranthene and pyrene on soot (calculated using specific surface area) was estimated to be near 5×10^{-3} at $T = 310$ K.

1. Introduction

Polycyclic aromatic hydrocarbons (PAHs), which principally originate from incomplete combustion and pyrolytic processes at high temperatures, are recognized as important pollutants with carcinogenic and mutagenic properties.[1] Partitioning of PAHs between particulate and gas phases is a very important factor determining the atmospheric fate of these compounds (transport, reactivity, deposition processes) as well as their health and climate impact and their influence on chemical composition of the atmosphere.[1−3]

The distribution of PAHs between the two phases depends on the physicochemical properties of PAH (saturation vapor pressure), those of the particulate phase (surface area, composition), and on the environmental conditions (temperature). This distribution is usually described by a partition coefficient K_P (m^3 μg^{-1}):[4−6]

$$K_P = \frac{(F/\mathrm{TSP})}{A}$$

where A and F (in ng m^{-3}) are equilibrium concentrations in the gas and particulate phase, respectively, and TSP (in μg m^{-3}) is the total suspended particulate matter.

Gas−solid adsorptive partitioning theory predicts that:[5]

$$K_P = \frac{N_S a_{\mathrm{TSP}} T\, e^{(\Delta H_{des} - \Delta H_{vap})/RT}}{1600 P_L^{\circ}} \qquad (1)$$

where N_S is the concentration of surface adsorption sites (mol cm^{-2}); a_{TSP} is the specific surface area of the particulate matter (cm^2 μg^{-1}); ΔH_{des} and ΔH_{vap} are the enthalpies (kJ mol^{-1}) of desorption and vaporization, respectively; R is the molar gas constant; T is the temperature (K); and P_L° is the subcooled liquid vapor pressure (Torr). Assuming the value of $\Delta H_{des} - \Delta H_{vap}$ to be constant within a homologous series of molecules, this equation leads to a linear relationship between log K_P and log P_L°:

$$\log K_P = m \times \log P_L^{\circ} + b$$

which was widely used to interpret the PAHs partitioning observed under a variety of environmental conditions (for examples, see refs 7−10). The assumption of a constant value of $\Delta H_{des} - \Delta H_{vap}$ for PAH molecules is based on the field data of Yamasaki[4] analyzed by Pankow,[5] and to our knowledge it has never been systematically verified. The kinetic and thermodynamic data on the desorption of PAH from solid surfaces of atmospheric relevance is almost nonexistent, yet ΔH_{des} is a key parameter allowing direct calculations of K_P via eq 1 for given atmospheric aerosol loading (a_{TSP}) and using tabulated physicochemical parameters (ΔH_{vap}, P_L°) of the species of interest.

The present paper is the first one in a series on a systematic study of the kinetics and thermodynamics of a large set of PAH desorption from kerosene soot surface carried out in our laboratory. Soot particles being a coproduct of the incomplete combustion of fossil fuels and biomass represent an important source of PAHs as they contain high levels of these compounds. There were only a few laboratory studies dealing with the distribution of PAHs between gas phase and carbonaceous aerosol.[11−13] The work of Aubin and Abbatt,[13] where soot from the combustion of n-hexane was used as a model for atmospheric aerosols, seems to be the only one where the interaction of PAH with soot was realized with well-characterized solid support. However, it should be noted that only small PAHs (naphthalene, acenaphtylene, and acenaphtene), that is, most volatile compounds dominantly partitioned to the gas phase under atmospheric conditions, were considered.[13]

In the present paper we report the results from a kinetic study of the desorption of four-ring PAHs, fluoranthene, and pyrene,

* To whom correspondence should be addressed. Phone: +33 238255474; fax: +33 238696004; e-mail: bedjanian@cnrs-orleans.fr.
† ICARE.
‡ Ecole des Mines de Douai.

10.1021/jp803043s CCC: $40.75
Published on Web 10/01/2008

from soot. The experimental approach used in the study of PAH desorption from the laboratory generated soot samples is also detailed. It includes the procedures of soot production, extraction of PAHs from soot samples, and their concentration measurements as well as the employed kinetic method.

2. Experimental Section

Preparation of Soot Samples. A flat-flame burner used for the preparation and deposition of soot samples from premixed flames of liquid fuels was described in details previously.[14] It allowed for the generation of flames of high stability with known fuel/oxygen ratio. In the present study the mixture of hydrocarbons (decane/propylbenzene/propylcyclohexane = 74:15:11) were used as the fuel. This mixture (referred to as kerosene in the paper) was chosen as a proxy of kerosene as it well represents the combustion of kerosene,[15] and it facilitates soot preparation as it contains a small number of hydrocarbon constituents (with lower boiling point) compared with kerosene. Soot particles from stabilized premixed flame of this liquid fuel were sampled at different locations in the flame (from 1 to 7 cm above the burner surface) and were deposited on the outer surface of a Pyrex tube (0.9 cm o.d.), which was rotated on its axis and moved horizontally through the flame. Specific (BET) surface area and bulk density of the soot samples prepared and collected in this way were determined in previous studies from our group:[14,16] 120 ± 20 m^2 g^{-1} and $(3.6 \pm 0.7) \times 10^{-2}$ g cm^{-3}, respectively. The knowledge of the bulk density and of the mass and length of soot sample homogeneously distributed on the support tube allowed the determination of the soot coverage thickness.

Flow Reactor. Kinetics of soot-bound PAHs desorption was studied in a flow reactor combined with a modulated molecular beam mass spectrometer for detection of gaseous species.[14,16,17] The main reactor consisted of a Pyrex tube (45 cm length and 2.4 cm i.d.) with a jacket for the thermostatted liquid circulation (water or ethanol). Desorption experiments were carried out using a coaxial configuration of the flow reactor with movable triple central injector;[14,16,17] the outer tube of the injector served to protect the soot sample during its introduction into the reactor, and the inner one was used to provide a circulation of the thermostatted liquid inside the tube with soot sample. In such a way, the same temperature was maintained in the main reactor and on the soot surface during measurements of the PAHs desorption rate as a function of temperature.

Upon the soot sample being introduced into the reactor, kinetic measurements consisted of monitoring the concentrations of PAHs adsorbed on the soot surface as a function of desorption time (residence time in the reactor). Two methods were used for monitoring the kinetics of particulate PAHs desorption. The first one consisted in HPLC off-line concentration measurements of PAHs present in solvent extractions of soot samples corresponding to different desorption times. The second approach used in situ monitoring of the PAHs desorption kinetics by mass spectrometry with direct detection of the PAH molecules released into the gas phase from the soot surface. The two methods were complementary, the first one being appropriate for the measurements of the lower and the second one of the higher desorption rates, corresponding to characteristic times of a few tens minutes and of a few minutes, respectively.

Analysis of Particulate PAHs. Soot samples were extracted by means of an ultrasonic-assisted extraction method (optimized for PAH extraction from soot within the present study, see below), filtered, and analyzed for PAHs content using a Jasco high-performance liquid chromatograph. After injection of 20 μL of extract, compounds were separated on a 4.6 mm reverse phase C18 column (Uptispere 5TF, Interchim) using acetonitrile/water (flow gradient) as a mobile phase at a constant flow rate of 1 mL min^{-1}. The analytical column was preceded by a 4.6 mm reverse phase C18 guard column, and both columns were thermostatically controlled at 30 °C. PAHs were detected using multiwavelength Jasco MD-2010 UV/Visible and Jasco FP-2020 fluorescence detectors.

TABLE 1: List of Identified PAHs Present in Kerosene Soot Particles Produced in This Study, and Their Mean Concentrations (In μg Per mg of Soot)

PAH	abbreviation	detector[a]	concentration[b] (μg × mg^{-1})	concentration[c] (10^{-6} mol m^{-2})
phenanthrene	Phe	F	1.90 ± 0.13	0.089
anthracene	Ant	F	0.31 ± 0.03	0.015
fluoranthene	Flu	UV	3.58 ± 0.27	0.148
pyrene	Pyr	F	2.97 ± 0.25	0.122
benzo(ghi) fluoranthene	BghiF	UV	nc[d]	nc
acepyrene	AcP	F	nc	nc
benzo(a) anthracene	BaA	F	0.17 ± 0.01	0.006
chrysene	Chr	F	0.32 ± 0.02	0.012
benzo(e) pyrene	BeP	UV	0.83 ± 0.05	0.028
benzo(b) fluoranthene	BbF	F	0.57 ± 0.04	0.019
benzo(k) fluoranthene	BkF	F	0.13 ± 0.01	0.004
benzo(a)pyrene	BaP	F	0.92 ± 0.04	0.030
benzo(ghi) perylene	BghiP	F	1.83 ± 0.09	0.055
dibenz(ah) anthracene	DBahA	F	0.49 ± 0.02	0.015
indeno(1,2,3-cd) pyrene	IdP	UV	0.61 ± 0.03	0.018
anthanthrene	Antha	F	2.39 ± 0.14	0.072
coronene	Cor	F	1.29 ± 0.07	0.036

[a] F, fluorescence detector; UV, multiwavelength UV/Visible detector. [b] Error represents one standard deviation from mean value from five replicates. [c] Calculated using specific surface area of 120 m^2 g^{-1}.[14] [d] nc, not calibrated.

The PAHs present in kerosene soot particles and identified in the present study are reported in Table 1. Particulate PAH concentrations were quantified using calibrated solutions of PAH mixtures. The mean PAH concentrations of five replicates are given in Table 1. It was observed that the response of the two detectors used (fluorescence and UV/vis detectors) to the concentration of PAHs was linear in the range of PAH concentrations used in this study. Using the data presented in Table 1, a rough estimation of the soot coverage with PAH molecules can be made. The sum of the PAH concentrations presented in the last column of the Table is $\approx 0.7 \times 10^{-6}$ mol m^{-2}. This value can be compared with the values of 1.2×10^{-6} and 1.1×10^{-6} mol m^{-2} calculated for a maximum monolayer capacity of benz(a)anthracene and benzo(k)fluoranthene,[18] respectively; these compounds are the "mean" molecular weight PAHs in Table 1. Considering these data and the fact that not all compounds were detected and quantified, a near monolayer coverage with PAHs can be assumed for the soot samples studied in the present work.

Extraction of PAHs from Soot. The procedure of kinetic measurements employing off-line monitoring of the particulate PAHs with HPLC method required multiple analyses of PAH on the soot samples (at least 5−6 analyses per each desorption kinetics at each temperature), and consequently, needed both

high reproducibility of the particulate PAH measurements and a simple, efficient, and more-or-less rapid method for PAH extraction from soot samples. The extraction of natively soot-associated PAHs is a difficult task due to the strong sorption of these planar aromatic molecules to the graphitic surface of the carbonaceous particles. Extractions are commonly performed using ultrasonic, Soxhlet or more modern methods such as microwave, supercritical fluid, and accelerated solvent extraction (ASE). The Soxhlet extraction is the most widely used procedure, although it has some disadvantages: long extraction time (up to 20 h) and high cost and solvent consumption. Richter et al.[19] showed that the ASE technique, which combines elevated temperatures and pressures with liquid solvents, gives analyte recoveries equivalent to those obtained with Soxhlet and other techniques. The ASE method uses less solvent and takes significantly less time than the Soxhlet procedure. The comparability of ASE to Soxhlet extraction for determination of PAHs in a variety of environmental matrices was confirmed by Heemken et al.[20] and Schantz et al.[21] Moreover, it was observed that for diesel materials, the ASE technique was more efficient than Soxhlet extraction for the higher molecular weight PAHs.[22]

In the present study, we employed ultrasonic-assisted extraction using a high-intensity ultrasonic processor (Sonics VC750) combined with a sonotrode of 3 mm diameter to transmit the ultrasound into the liquid. The sample extraction with an ultrasonic processor is significantly faster compared with traditionally used ultrasonic bath due to higher and focused energy at the probe tip. The extractions were performed in a pulsation regime with sonication and relaxation cycles of 4 and 10 s, respectively. The pulse function avoids excessive heating of the solvent. A few series of experiments were carried out in order to choose appropriate solvent and to optimize the extraction conditions. In addition, specific experiments were conducted to check if the used method of ultrasonic extraction of soot-associated PAHs provides extraction efficiencies comparable to those of the ASE technique.

Extraction Solvent. Considering that the available data and recommendations from different studies comparing efficiencies of different solvents are conflicting and do not allow a single, best extractant for soot,[23] we have performed the ultrasonic extractions of PAHs from laboratory-generated kerosene soot using four different solvents: acetonitrile, methanol, dichloromethane, and toluene. Soot samples (2.5 mg) were loaded in 4 mL of solvent and were extracted in pulse regime with 4 s/10 s sonication/relaxation time and 3 min of total sonication time. The extracts were separated from soot particles using Teflon filters with pore diameter of 0.2 μm. Prior to HPLC analysis, the solvents were exchanged (if necessary) to acetonitrile. The results obtained in this series of experiments (Figure S1, Supporting Information) have shown that the extracting efficiencies of acetonitrile and toluene were higher (up to a factor 1.4) than those of methanol and dichloromethane, particularly for heavier PAHs. Acetonitrile was preferred and was used as extraction solvent throughout the present study since it was used as a mobile phase (flow gradient with water) in HPLC analysis of the extracts. This simplified the protocol of PAHs analysis by elimination of the solvent exchange stage.

Extraction Conditions. To optimize the extraction procedure, two parameters were varied: the extraction time and soot sample mass to solvent volume ratio. It was observed that the concentrations of extracted PAHs obtained with total sonication times between 1.5 and 8 min were very similar (within 10%). The sonication time of 3 min was then selected as a suitable time for extraction of PAHs by the method used. This corresponds to the total time of the extraction procedure (sonication + relaxation) of nearly 10 min. Comparison of the PAH content of the extracts of soot samples of the same mass (3 mg) obtained with different volumes of extraction solvent (2, 4, 6, and 10 mL of acetonitrile) has not revealed any significant difference, although the concentrations of all compounds obtained with 2 mL of the solvent seemed to be the lowest in the series. Finally, the soot mass being lower than 3 mg for most of the samples used in the kinetic study, the extraction solvent volume of 4 mL was regularly used.

Extraction Efficiency. To evaluate the extraction efficiency of the method and a possible loss of the PAHs during soot/solvent filtration, three successive extractions of the same soot sample (last two extractions with soot remaining on the Teflon filter) were carried out. Analysis of the observed data (Table S1, Supporting Information) has shown that at least 90% of extractable concentrations of PAHs were successfully extracted during the first extraction.

Comparison with ASE Technique. Soot samples of approximately 5 mg were mixed with clean sand, loaded into the 33 mL extraction cell, and extracted with acetonitrile, dichloromethane, toluene/methanol (volume ratio = 1), or acetone/hexane (volume ratio = 1) using accelerated solvent extraction (ASE 200 Dionex) under 100 bar pressure and at a temperature of 120 °C. A 5 mL portion of extract was exchanged to acetonitrile, concentrated to 1 mL by evaporation with a gentle stream of N_2, and processed for PAH measurements with HPLC. Two observations could be made from the results of these experiments obtained with three replicates for each solvent. First, no significant difference was observed between the ASE extractions performed with different solvents. This observation is in line with the results of Schantz et al.,[21] where the concentrations of PAHs determined with the ASE method and three different solvents (methylene chloride, toluene, and toluene/methanol (volume ratio = 1)) for extraction of PAHs from diesel particulate matter (SRM 1650) were found to be comparable. Second, for the soot samples used and PAHs identified and monitored in the present study, the extraction efficiency of the ultrasonic method was, in general, very close to that of ASE.

Influence of Combustion and Soot Deposition Conditions on Concentrations of Particulate PAHs. As indicated above, a part of the kinetic study of soot-bound PAH desorption consisted of the off-line concentrations measurements of particulate PAHs as a function of desorption time (residence time in the flow reactor). This procedure required each kinetic point (corresponding to a given desorption time) to be measured with a newly prepared soot sample. It means that to carry out correct kinetic measurements it was necessary to have initially identical soot samples, that is, similar initial concentrations and homogeneous distribution of PAHs through the soot bulk. To ensure stability and reproducibility of particulate PAH concentrations produced over the flat flame burner used in this study, we have carried out a few series of test experiments where the influence of combustion and soot deposition conditions on soot PAHs content was studied.

Flame Richness. Flame richness is a key parameter determining the rate of soot formation. The objective of these experiments was to check if slight variations of the flame richness during soot collection could significantly influence the concentrations of PAHs adsorbed on the soot surface. Soot samples from the premixed flames with richness values (fuel/oxygen ratio multiplied by stoichiometric coefficient of oxygen) of 1.9, 1.95, 2.0, 2.1, and 2.15 were collected and analyzed

(Figure S2, Supporting Information). No dependence of particulate PAH concentrations on flame richness was observed in the range of 15% uncertainty (experimental uncertainty on the protocol of PAHs concentration determination). Soot samples formed in the flames with a richness near 2.0 were used throughout the present study.

Sampling Height above the Burner. Soot PAHs content was determined as a function of soot sampling height above the burner plate. No systematic trend was observed in PAH concentrations by sampling at different heights (1, 2.5, 4, and 7 cm), although the concentrations of some compounds significantly differed from the mean value of four measurements (especially at extreme sampling positions of 1 and 7 cm). All the desorption experiments described below were carried out with soot sampled at 4 cm height above the head of the burner.

Support Tube Temperature. As discussed above, soot samples were collected on Pyrex tubes, which were rotated and moved horizontally through the flame. With this configuration, the part of soot sample which is moved out of the flame zone remains exposed to the gas-phase combustion products, in particular, to the gas-phase PAHs. Thus, the concentrations of particulate PAHs, which are expected to be in equilibrium with those in the gas phase, are defined by the temperature of the soot substrate. Considering the relatively high adsorption energies of PAHs to soot, one can expect that even a slight variation of this temperature can significantly influence the concentrations of some adsorbed PAHs. Our first experiments on soot production and PAHs content analysis have effectively revealed instability in concentrations of light PAHs from one experiment to another. To solve this problem, the support tube was thermostabilized by circulating thermostatted heated water inside this tube. This allowed us to obtain soot samples with reproducible PAHs content. Another advantage of this configuration is that it avoided condensation of combustion-produced water on soot samples.

Soot sample PAHs content was also studied as a function of the temperature of thermostatted water circulating inside the soot support tube (Figure S3, Supporting Information). As expected, the concentrations of smaller PAH molecules (phenanthrene−chrysene) decreased with increasing temperature. The concentrations of heavier PAHs were independent of the temperature of thermostatted liquid in the temperature range used (45−80 °C). We have chosen the temperature of 45 °C for soot preparation throughout this study. At lower temperatures it was difficult to obtain homogeneous soot coverage due to water condensation on the support tube.

Reproducibility of Soot-bound PAHs Content. A specific series of tests was conducted to establish the repeatability of the overall soot production and analysis protocol: flame conditions, soot collection, soot mass measurements, extraction, filtration, and HPLC analysis. The five soot samples were prepared under identical combustion and soot deposition conditions, extracted, and analyzed for PAHs using the protocol described above. The deviations of the concentrations of individual compounds in the five different soot samples from mean value of these five measurements were found to be, in general, within a few percents and did not exceed 15% (Figure S4, Supporting Information).

PAH Concentration As a Function of Soot Coverage Thickness. To check if the adsorbed PAHs on soot surface are homogeneously distributed throughout the bulk of soot, the soot sample PAHs content was studied as a function of the thickness of soot coating. Examples of the observed dependencies are shown in Figure 1, where particulate PAH concentrations are presented as a function of the mass of soot deposited per unit length of the support tube, which is equivalent to the dependence on the thickness of soot coating. Error bars presented for illustration for one compound correspond to 15% uncertainty on the measurements of PAH concentrations and 3−10% uncertainty (depending on mass) on the measurements of soot mass. The observed linear increase of PAH concentrations with increasing soot coverage thickness indicates a homogeneous PAHs distribution through the whole volume of soot samples.

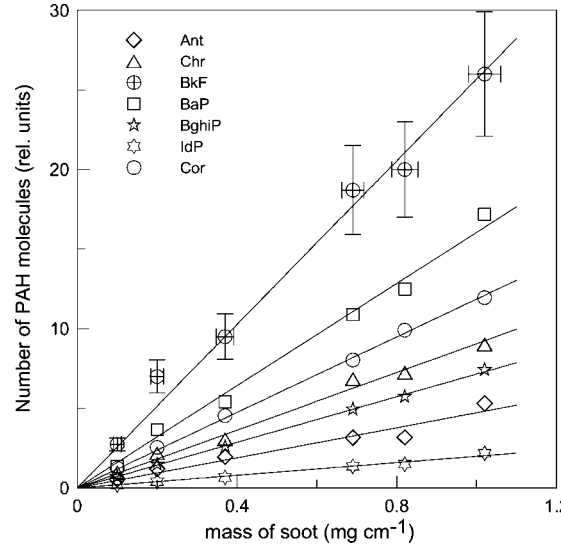

Figure 1. Number of soot-bound PAH molecules (per 1 cm of soot sample length) as a function of the mass of soot sample (per 1 cm of soot sample length). For PAH abbreviations see Table 1.

3. Results and Discussion

Fresh soot samples were used in all kinetic experiments. It was first verified that the PAH surface concentrations did not significantly change (due to desorption or photochemical degradation) during soot sample handling (10−20 min) between its preparation and introduction into the flow reactor. The experiments showed no significant changes in PAH concentrations during up to 1 h exposure of the soot samples to air under ambient laboratory conditions ($T = 298 \pm 3$ K).

Kinetics of PAHs Desorption. Example of experimental plots of particulate pyrene and fluoranthene desorption measured in the flow reactor for long residence times and at low pressure (≤0.1 torr of He) is shown in Figure 2. An important observation is that the kinetics are reaching a plateau, that is, a part of sorbed PAHs is remaining on the soot surface and is not released into the gas phase even at fairly long pumping times (near 17 h). The number of PAH molecules remaining on the surface was found to be dependent on soot sample temperature. As one could expect, the plateau level is decreasing with increasing temperature (Figure 3).

To obtain additional information on this incomplete PAHs desorption, the decay rates of particulate PAHs were measured as a function of the mass of soot deposited per unit length of the support tube, which is equivalent to the dependence on the thickness of the soot coating. An example of results obtained for desorption of pyrene is presented in Figure 4. The thickness of soot coverage was largely varied (up to a factor 17). Two main observations can be made from the data presented in Figure 4. First, there is a clear negative dependence of the desorption rate on the mass of soot sample. This effect can be attributed to the occurrence of a readsorption process that takes place at

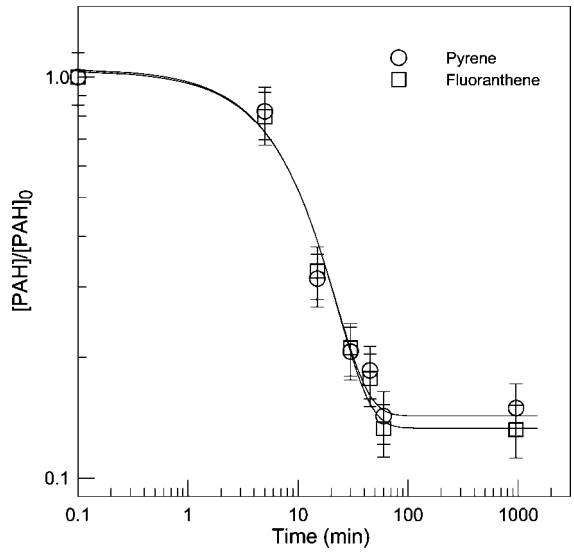

Figure 2. Kinetics of soot-bound pyrene and fluoranthene desorption measured in the low-pressure flow reactor at long desorption times (T = 300 K). The solid lines represent the plateau-approaching exponential funtion fit to the experimental points.

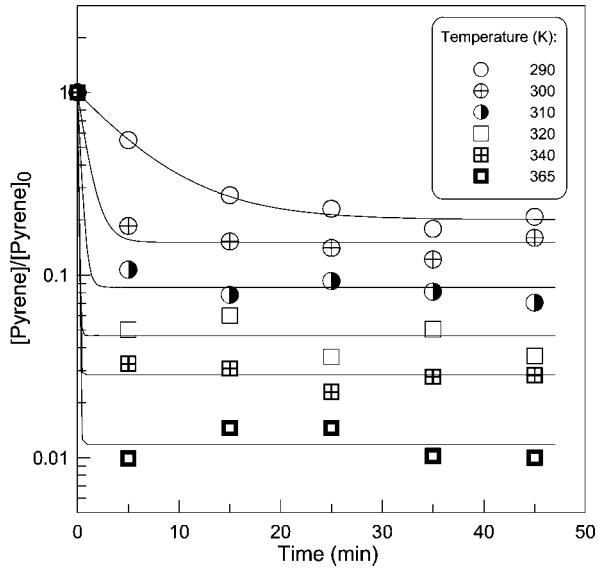

Figure 3. Kinetics of soot-bound pyrene desorption: dependence of the plateau level on temperature. The solid lines are drawn to guide the eye.

low flow velocities in the reactor and when the total mass of soot sample is relatively high (see discussion on readsorption process in the next section). The second important observation is that the plateau level in Figure 4 is independent of the thickness of the soot coating. It means that PAHs are desorbing homogeneously from the soot surface and that the concentration of the non-desorbed PAH molecules remaining on the soot surface is similar throughout the soot sample volume. This observation seems to indicate that the radial diffusion of PAHs from deeper soot layers (to outer soot surface) is not responsible for the observed plateau, and the incomplete recovery is most probably caused by the PAH molecules trapped in nanopores of soot. It can be noted that similar effect of incompleted degradation of particulate PAHs was observed in studies of heterogeneous reactions of PAHs adsorbed on diesel particulate exhaust[24] and graphite particles[25] with atmospheric gaseous oxidant species (NO_2, OH,[24] and O_3[25]). This observation was

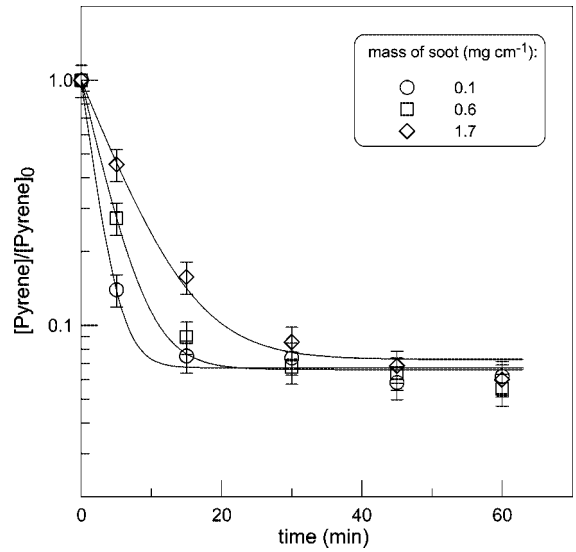

Figure 4. Kinetics of soot-bound pyrene desorption at T = 315 K as a function of soot coverage thickness. Total mass of soot samples: ○, 1 mg; □, 3.5 mg; ◇, 5 mg: flow velocity in the reactor, 780 cm s^{-1}.

attributed to possible housing of PAHs in pores, leading to their limited accessibility to the oxidant species.[24]

The other possibile explaination for the observed incomplete desorption of PAHs could be the existence of different types of sorption sites with different adsorption energies. However, that seems to be less probable, considering the shape of the desorption kinetic curves, particularly in the plateau region, as a function of temperature (Figure 3). Effectively, in the case of an energetically multisite soot surface, at sufficiently high temperatures one might expect biexponential kinetics for desorption of PAHs: rapid desorption from the first type of active sites (generally more than 70% of the initial concentration of PAHs) followed by more-or-less rapid (depending on temperature) PAHs desorption from the "strong" active sites. This type of kinetics has never been observed even though the temperature was changed across a wide range (Figure 3).

Finally, in the study of the PAHs desorption, the plateau region (i.e., undesorbed molecules) was not considered when determining the desorption rate constants. At low desorption rates the experimental plots could be reasonably described by a first-order kinetics. In this case, the first-order rate coefficients were determined from the exponential fits to the experimental plots:

$$[\mathrm{PAH}] = [\mathrm{PAH}]_0 \times \exp(-k_{\mathrm{des}} t)$$

When it was necessary to take into account the existence of the plateau, the kinetics were fitted with an exponential function approaching the plateau:

$$[\mathrm{PAH}] = [\mathrm{PAH}]_{\mathrm{plateau}} + ([\mathrm{PAH}]_0 - [\mathrm{PAH}]_{\mathrm{plateau}}) \exp(-k_{\mathrm{des}} t)$$

In these expressions $[\mathrm{PAH}]_0$, $[\mathrm{PAH}]$, and $[\mathrm{PAH}]_{\mathrm{plateau}}$ are particulate PAH concentrations at $t = 0$, t and at the plateau region, respectively. Thus, undesorbed molecules were not considered when determining the first-order rate constant.

Readsorption of PAHs to Soot. Under flow conditions the PAH molecules desorbed from the soot surface can readsorb to soot or to be evacuated with the flow of the carrier gas (helium in the present study). The adsorption rate can be expressed as follows;

$$R_{\mathrm{ad}} = k_{\mathrm{ad}}(1-\theta)[\mathrm{PAH}]_{\mathrm{gas}}$$

where k_{ad} is the adsorption rate constant, and θ = [PAH]/$[\mathrm{PAH}]_0$is the soot surface coverage with PAH. To reduce the

rate of the readsorption, one needs to reduce the gas-phase concentration of PAH. This can be achieved by two ways. The first one is a simple dilution of the desorbed PAH with the carrier gas that, under flow conditions at a given pressure in the reactor, is equivalent to an increase of the flow rate. The second way consists in reducing of the absolute number of PAH molecules ejected into the gas phase from the soot surface. This can be achieved by decreasing the initial total number of particulate PAH molecules introduced into the reactor by a reduction of the total mass of soot sample. This in turn has been achieved by reduction of the soot sample length or/and soot sample coating thickness.

To establish the experimental conditions where the readsorption process could be neglected, a few series of test experiments were carried out. In these experiments the desorption of fluoranthene and pyrene was studied under varied experimental conditions (total pressure and flow rate in the reactor and soot sample mass, length, and thickness) using mass spectrometric detection of the sum of their concentrations in the gas phase (sum of peak intensities at $m/z = 202$). The study of the desorption kinetics of these two species using the sum of their relative concentrations is justified since the desorption rate constants of these two PAHs from soot are similar within experimental uncertainty (see below). The test experiments consisted of introducing the support tube with soot sample into the thermostatted ($T = 310$ K) flow reactor and monitoring the concentrations of pyrene and fluoranthene desorbed from the soot surface. In these experiments, direct in situ detection of the PAHs desorption kinetics by mass spectrometry was preferred to that using off-line analysis of the species with HPLC method. The quality of the measurements by the two methods are equivalent, but kinetic experiments combined with HPLC analysis are very time-consuming: a few hours per kinetics including a preparation of 5−6 soot samples per kinetics and their respective extraction, filtration, and HPLC analysis. In addition, the procedure of the kinetic measurements with off-line analysis of the surface-bound species is not adapted for the measurements of rapid processes. Therefore, the approach using the direct detection of the desorbed species by mass spectrometry was more appropriate to carry out the multiple test experiments needed, since it allows the monitoring of rapid (few minutes) desorption kinetics using only one soot sample per kinetics.

Figure 5a shows a typical behavior of the intensity of the mass spectrometric signal at $m/z = 202$ following the introduction ($t = 0$ min) of the soot sample into the flow reactor. Fast initial desorption of the PAHs is followed by a decrease of the desorption rate due to reduction of the particulate PAH concentrations. Integration of the curve in Figure 5a within a given time interval allows the calculation of the corresponding number of PAH molecules desorbed from the soot surface, Δ[PAH]. Assuming an exponential decay of particulate PAH concentrations:

$$\Delta[\mathrm{PAH}] = [\mathrm{PAH}]_0 - [\mathrm{PAH}] = [\mathrm{PAH}]_0(1-\exp(-k_{\mathrm{des}}t)) \quad (2)$$

where $[\mathrm{PAH}]_0$ and [PAH] are the concentrations of particulate PAH at desorption times 0 and t, respectively. The integrated data from Figure 5a are shown in Figure 5b. The fit to the experimental points (solid line in Figure 5b) according to the eq 2 allows for the determination of the desorption rate constant k_{des}.

All the results obtained for k_{des} by this method under different experimental conditions are shown in Figure 6 as the dependence of the desorption rate on the combined empirical parameter

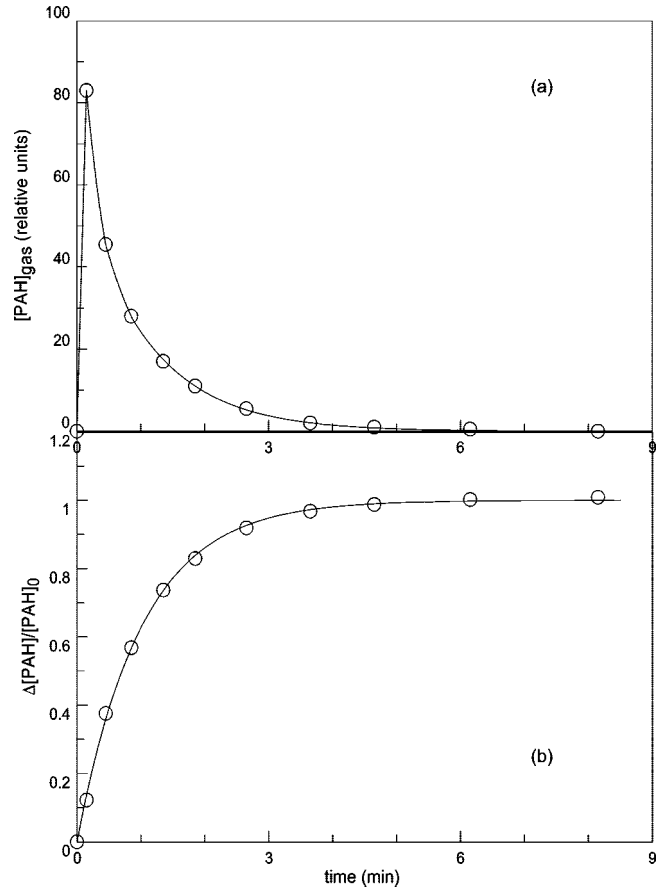

Figure 5. Mass spectrometric monitoring (at $m/z = 202$) of the desorption of fluoranthene and pyrene from soot surface at $T = 310$ K: (a) sum of the gas phase concentrations of the desorbed fluoranthene and pyrene as a function of desorption time (solid line is drawn to guide the eye); (b) fraction of PAHs (fluoranthene + pyrene) molecules desorbed from the soot surface as a function of desorption time.

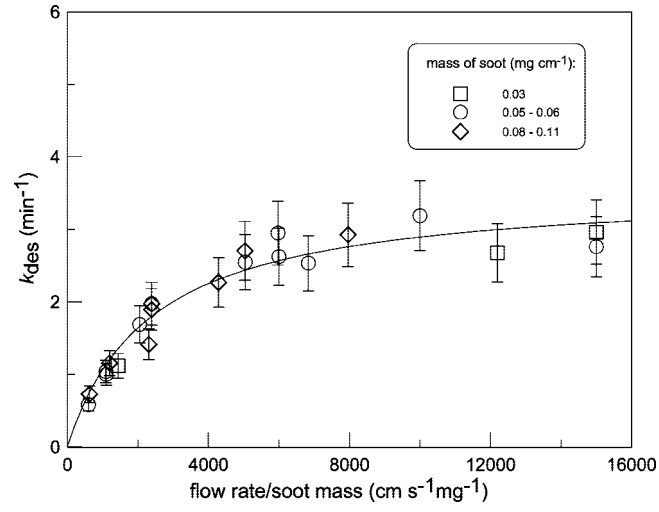

Figure 6. Combined desorption rate of soot-bound fluoranthene and pyrene at $T = 310$ K from different soot samples and under different experimental conditions (see text) as a function of flow rate to soot sample mass ratio. The error bars represent a 15% uncertainty on k_{des}. The solid line is a fit of the experimental data with eq 2.

representing the ratio of flow velocity (in cm s^{-1}) to soot sample mass (in mg). These two parameters were largely varied: soot sample total mass in the range 0.2−1.3 mg and flow velocity in the range 360−3980 cm s^{-1}. As expected, the impact of readsorption of PAHs to soot on the measured values of their

desorption rate is more important at lower flow rates and higher masses of soot samples. The data of Figure 6 indicate that for the flow rate to soot mass ratios higher than 6000 cm s^{-1} mg^{-1} the measured value of k_{des} can be considered as independent of this parameter, that is, the possible contribution of PAHs readsorption processes can be neglected. It means that to correctly measure the k_{des}, for example at a flow rate of 3000 cm s^{-1} in the reactor, one should use soot samples with masses lower than 0.5 mg. In the present study, all the measurements of the desorption rate of PAHs from soot surface were carried out using flow rates of 3000−4300 cm s^{-1} and total mass of soot samples between 0.2 and 0.4 mg.

The data presented in Figure 6 were obtained at total pressure of 0.2−1.0 torr of helium in the reactor and with soot samples of different length (2.7−14.9 cm) and of different thickness, corresponding to 0.03−0.11 mg of soot per 1 cm of the support tube. The measured values of the desorption rate were found to be independent of these parameters under these conditions. Independence of PAHs desorption kinetics on soot coverage thickness is an important point, because it seems to indicate that PAHs diffusion from underlying soot layers is not a limiting factor in the measurements of the PAHs desorption rate under these experimental conditions.

The data presented in Figure 6 allow for a rough estimation of the uptake coefficient (γ) of the PAHs on soot surface. Considering a simplified mechanism where desorbed molecules would be either readsorbed to soot surface (k_{ads}) or removed from the reaction zone (defined by soot sample length, L) by the flow of bath gas (flow velocity v), the measured rate of PAHs desorption can be approximated using the following expression:

$$k_{des}^{meas} = k_{des}\left(1 - \frac{k_{ads}}{k_{ads} + \frac{2v}{L}}\right)$$

where $L/2v$ is a mean residence time of PAHs in the reaction zone. k_{ads} is related to γ through the following expression:

$$k_{ads} = \frac{\omega\gamma}{4}\frac{S}{V}$$

where ω is the average molecular speed, V is the volume of the reaction zone, and S is the surface area of the soot sample. Considering that $V = 3.8$ cm^2 $\times$ L (surface area between soot sample tube and main reactor multiplied by soot sample length), $S = 1200$ cm^2 mg^{-1} $\times$ m (specific BET surface area of soot sample of mass m in mg) and $\omega = 11922$ cm s^{-1}, one gets: $k_{ads} = 9.4 \times 10^5\ \gamma m/L$, and

$$k_{des}^{meas} = k_{des} \times \left(1 - \frac{\gamma}{\gamma + 2.1\times10^{-6} v/m}\right) \qquad (3)$$

The best fit of the experimental data with this expression (solid line in Figure 6) provides a value of $\gamma \approx 0.005$ for the combined uptake coefficient of fluoranthene and pyrene on soot surface at $T = 310$ K.

Fluoranthene and Pyrene Desorption Rate As a Function of Temperature. Examples of kinetic runs for desorption of fluoranthene from soot surface measured at different temperatures are shown in Figure 7. Continuous lines represent the simple exponential (T = 260, 265, and 270 K) or plateau-approaching exponential (T = 275 and 280 K, according to eq 2) function fits to the experimental data that were used to derive the values of the desorption rate constant (k_{des}) at different temperatures. The experimental uncertainty of k_{des}, in general, was estimated to be within 15−25%. However, it could be much higher (up to 50%) for the lowest desorption rates measured, corresponding to a few percents decrease of the particulate PAH concentration.

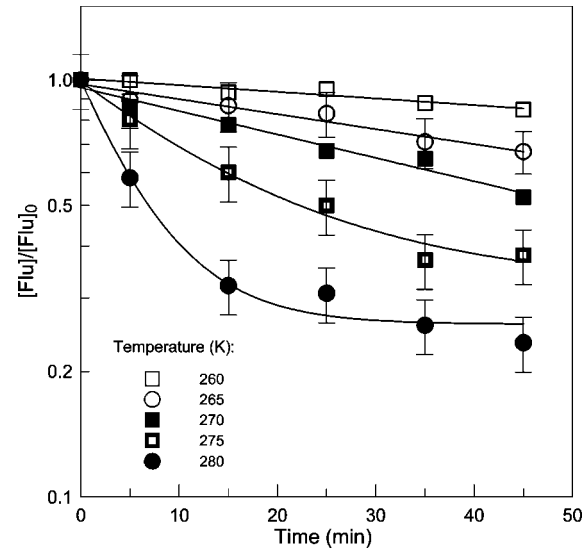

Figure 7. Kinetics of soot-bound fluoranthene desorption at different temperatures.

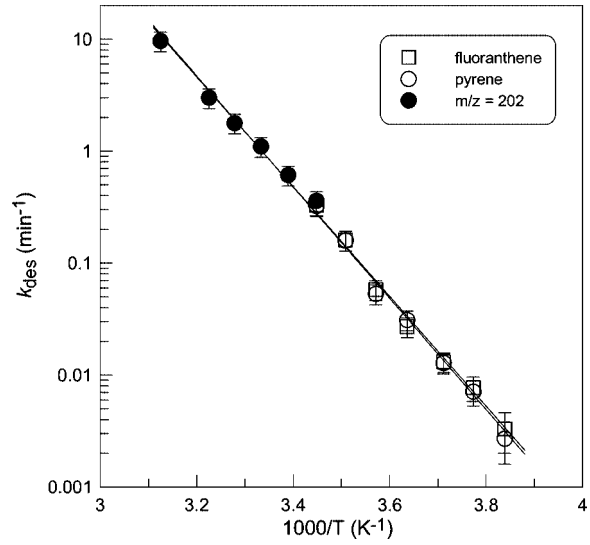

Figure 8. Temperature dependence of the desorption rate constants of soot-bound pyrene and fluoranthene. Open symbols: data from off-line HPLC separate detection of the particulate pyrene and fluoranthene; filled circles: data from gas phase mass spectrometric monitoring of the desorbed species at m/z = 202 (see text).

Temperature dependence of the desorption rate constant was described by the Arrhenius equation:

$$k_{des} = k_0 \exp(-E_A/RT)$$

where k_0 is the pre-exponential frequency factor, E_A is the activation energy for desorption, and R is the molar gas constant. Temperature dependences of k_{des} observed for pyrene and fluoranthene in the temperature range 260−320 K are shown in Figure 8. One can note a very good agreement between the results obtained by the two different approaches used for the measurements of k_{des}: in situ mass spectrometric detection of the desorbed PAHs in the gas phase (rapid desorption) and off-line analysis of the particulate PAH concentrations (slow desorption). Continuous lines in Figure 8 represent the best Arrhenius expression fit to the experimental data and yield the following expressions for the desorption rate constants (in s^{-1}):

$$k_{des} = 4 \times 10^{14} \exp[(-93900 \pm 1700)/RT)]$$

$$k_{des} = 6 \times 10^{14} \exp[(-95200 \pm 1800)/RT)],$$

for fluoranthene and pyrene, respectively, with a factor of 2 uncertainty on the pre-exponential factors and 1σ statistical uncertainties quoted for the activation energies (in J mol^{-1}).

The data obtained in the present study for the desorption activation energies can be compared with the sublimation enthalpies of the corresponding species, 98.3 and 97.9 kJ mol^{-1},[26] for fluoranthene and pyrene, respectively. These enthalpies are relevant to binding energy for desorption from PAH multilayer coverage or when the activation energies for desorption from monolayer and multilayer coverage are similar.[27] One can note that measured activation energies are quite close to the corresponding sublimation enthalpies. The similarity of these values seems to reflect the structural resemblance between planar PAH molecules and graphitic sheets of soot and the similar physical nature of the PAH−PAH and PAH−soot interactions.

4. Summary and Conclusion

The experimental approach for the measurements of PAHs desorption from the laboratory-generated soot samples, reported in detail in this work, has been first applied to fluoranthene and pyrene. The thermal desorption kinetics of these two PAHs from kerosene soot surface, studied over the temperature range 260−320 K yielded Arrhenius expressions for the desorption rate constants with activation energies ($\pm 1\sigma$) of 93.9 ± 1.7 and 95.2 ± 1.8 kJ mol^{-1} for fluoranthene and pyrene, respectively. The combined uptake coefficient of fluoranthene and pyrene on soot (calculated using specific surface area) was estimated to be near 5×10^{-3} at $T = 310$ K.

An extended discussion on a trend in the ordering of PAHs with respect to the desorption thermodynamics and on the atmospheric applications to the partitioning of these compounds between solid and gas phase requires the desorption enthalpies data for a large set of PAHs. In this respect, experiments using the experimental protocol developed in the present study are currently under way in our laboratory to determine the kinetic parameters for three- to six-ring PAHs desorption from soot surface.

Acknowledgment. This study has been carried out within the program PRIMEQUAL 2, funded by French Ministry of Ecology and Sustainable Development. A.G. is very grateful to Ecole des Mines de Douai and European Structural Funds for cofinancing her Ph.D. grant.

Supporting Information Available: Relative concentrations of selected PAHs from three successive ultrasonic extractions of soot sample (Table 1S); soot-bound PAHs ultrasonic-assisted extractions with different solvents (Figure 1S); concentrations of soot-bound PAHs as a function of flame richness (Figure 2S) and support tube temperature (Figure 3S); repeatability of the protocol used for soot production, collection and surface-bound PAHs analysis (Figure 4S). This material is available free of charge via the Internet at http://pubs.acs.org.

References and Notes

(1) Finlayson-Pitts, B. J.; Pitts, J. N. J. *Chemistry of the Upper and Lower Atmosphere: Theory, Experiments and Applications*; Academic Press: San Diego, 2000.
(2) Calvert, J. G.; Atkinson, R.; Becker, K. H.; Kamens, R. M.; Seinfeld, J. H.; Wallington, T. J.; Yarwood, G. *The Mechanisms of Atmospheric Oxidation of Aromatic Hydrocarbons.*; Oxford University Press: New York, 2002.
(3) Bidleman, T. F. *Environ. Sci. Technol.* **1988**, *22*, 361.
(4) Yamasaki, H.; Kuwata, K.; Miyamoto, H. *Environ. Sci. Technol.* **1982**, *16*, 189.
(5) Pankow, J. F. *Atmos. Environ.* **1987**, *21*, 2275.
(6) Pankow, J. F. *Atmos. Environ. Part A. General Topics* **1991**, *25*, 2229.
(7) Gustafson, K. E.; Dickhut, R. M. *Environ. Sci. Technol.* **1997**, *31*, 140.
(8) Simcik, M. F.; Franz, T. P.; Zhang, H.; Eisenreich, S. J. *Environ. Sci. Technol.* **1998**, *32*, 251.
(9) Ngabe, B.; Poissant, L. *Environ. Sci. Technol.* **2003**, *37*, 2094.
(10) Sitaras, I. E.; Bakeas, E. B.; Siskos, P. A. *Sci. Total Environ.* **2004**, *327*, 249.
(11) Niessner, R.; Wilbring, P. *Anal. Chem.* **1989**, *61*, 708.
(12) Hueglin, C.; Paul, J.; Scherrer, L.; Siegmann, K. *J. Phys. Chem. B* **1997**, *101*, 9335.
(13) Aubin, D. G.; Abbatt, J. P. *Environ. Sci. Technol.* **2006**, *40*, 179.
(14) Lelièvre, S.; Bedjanian, Y.; Pouvesle, N.; Delfau, J. L.; Vovelle, C.; Le Bras, G. *Phys. Chem. Chem. Phys.* **2004**, *6*, 1181.
(15) Dagaut, P. *Phys. Chem. Chem. Phys.* **2002**, *4*, 2079.
(16) Bedjanian, Y.; Lelièvre, S.; Le Bras, G. *Phys. Chem. Chem. Phys.* **2005**, *7*, 334.
(17) Lelièvre, S.; Bedjanian, Y.; Laverdet, G.; Le Bras, G. *J. Phys. Chem. A* **2004**, *108*, 10807.
(18) Werner, D.; Karapanagioti, H. K. *Environ. Sci. Technol.* **2005**, *39*, 381.
(19) Richter, B. E.; Jones, B. A.; Ezzell, J. L.; Porter, N. L.; Avdalovic, N.; Pohl, C. *Anal. Chem.* **1996**, *68*, 1033.
(20) Heemken, O. P.; Theobald, N.; Wenclawiak, B. W. *Anal. Chem.* **1997**, *69*, 2171.
(21) Schantz, M. M.; Nichols, J. J.; Wise, S. A. *Anal. Chem.* **1997**, *69*, 4210.
(22) Turrio-Baldassarri, L.; Battistelli, C. L.; Iamiceli, A. L. *Anal. Bioanal. Chem.* **2003**, *375*, 589.
(23) Jonker, M. T. O.; Koelmans, A. A. *Environ. Sci. Technol.* **2002**, *36*, 4107.
(24) Esteve, W.; Budzinski, H.; Villenave, E. *Atmos. Environ.* **2006**, *40*, 201.
(25) Perraudin, E.; Budzinski, H.; Villenave, E. *J. Atmos. Chem.* **2007**, *V56*, 57.
(26) Nass, K.; Lenoir, D.; Kettrup, A. *Angew. Chem., Int. Ed. Engl.* **1995**, *34*, 1735.
(27) Ulbricht, H.; Zacharia, R.; Cindir, N.; Hertel, T. *Carbon* **2006**, *44*, 2931.

JP803043S